Shape and Substructure of Skeletal Muscle Myosin Light Chain Kinase†

Georg W. Mayr and Ludwig M. G. Heilmeyer, Jr.*

ABSTRACT: To evaluate the shape and substructure of calmodulin-dependent myosin light chain kinase from skeletal muscle, the apo- and holoenzyme and three well-characterized proteolytic fragments were studied by enzymatic measurements, by hydrodynamic techniques, and by CD spectroscopy. For the native apoenzyme, a molecular weight of 70 300 was established by sedimentation equilibrium in contrast to >80 000 estimated by electrophoresis. A highly asymmetric structure was evidenced from sedimentation and viscosity data. Examination of two slightly different calmodulin binding fragments of M_r ~36 000 showed that both are fairly globular, high in α-helix content, enzymatically active, and calmodulin regulated. They have been termed head fragments. The third fragment of M_r ~33 000 could be demonstrated to represent the remaining part of the native enzyme by its amino acid composition and CD spectrum. This enzymatically inactive fragment, although low in α-helix content and rich in proline, was shown to be highly asymmetric ($a/b > 10$). From the latter, termed tail fragment and one of the head fragments, a more active enzyme could be partially reconstituted. Modeling by spherical beads [Bloomfield, V., Dalton, W. O., & Van Holde, K. E. (1967) *Biopolymers 5*, 135–148] led to a close agreement in observed and calculated frictional ratios for all fragments as well as the apoenzyme built up by end to end arrangement of head and tail fragment, suggesting this headed structure for the enzyme. Holoenzyme formation by calmodulin binding to the head was accompanied by an increase in asymmetry and α-helix content and a decrease in apparent partial specific volume.

Phosphorylation of myosin at light chain 2 by myosin light chain kinase (MLCK)[1] is widely accepted to play an essential role in the Ca^{2+}-mediated activation of smooth muscle contraction (Sobieszek & Small, 1977; Walsh et al., 1982c) as well as in myosin assembly (Suzuki et al., 1978). In striated muscle the role of MLCK is not yet elucidated as clearly (Bârány et al., 1980); Crow & Kushmerick, 1982; Cooke et al., 1982). Most of the MLCK species isolated require calmodulin for their activity expression (Yazawa & Yagi, 1977; Dabrowska et al., 1978). Calmodulin (CM) reversibly binds to MLCK with high affinity in a calcium-dependent manner (Crouch et al., 1981).

Molecular weights between 77 000 and 94 000 for the striated muscle MLCK (Pires & Perry, 1977; Wolf & Hofmann, 1980; Edelman & Krebs, 1982) and between 105 000 and 155 000 (Dabrowska et al., 1977; Adelstein & Klee, 1981; Walsh et al., 1982b) for the smooth muscle MLCK were found by gel electrophoresis in the presence of $NaDodSO_4$.

Hydrodynamic data have been collected for the smooth muscle enzyme (Adelstein & Klee, 1981), and some data also exist on striated muscle MLCK (Crouch et al., 1981). But whereas much information on the enzymatic function and regulatory role of MLCK has been accumulated, little is known about structural details of MLCK and their relevance.

Here, the hydrodynamic reexamination of the molecular weight of the skeletal muscle enzyme indicates a lower molecular weight than previously reported. As the major object of this study, data on the overall shape and secondary structure as well as on functionally relevant substructures of the apoenzyme and holoenzyme (i.e., the complex with CM) were collected from native MLCK, three well-characterized proteolytic fragments, and their corresponding complexes with CM. Hydrodynamic techniques, far-UV CD spectroscopy, and enzymatic measurements were employed. A model of MLCK is proposed, the major feature being a head-and-tail structure with the head containing all the domains essential for activity.

Materials and Methods

Chemicals and Reagents. Fluphenazine dihydrochloride was a generous gift of Heyden GmbH, Munich, FRG, divinyl sulfone and 1,4-butanediol diglycidyl ether were from EGA-Chemie, FRG, [^{32}P]phosphoric acid was from New England Nuclear, and [γ-^{32}P]ATP was prepared according to Glynn & Chappel (1964). DEAE-cellulose DE-52 and filter disks (GFC, 2 cm) were from Whatman, and DEAE-Sephacel, Sephacryl S-300, Sephadex G-25, and Sepharose 4B were from Pharmacia. Crystallized bovine serum albumin and TPCK-treated trypsin (from bovine pancreas) were from Serva, FRG, and soybean trypsin inhibitor and ATP were from Boehringer Mannheim, FRG. Bio-Gel HTP (hydroxyapatite) was from Bio-Rad. All other reagents were of analytical grade. Special buffers used were the following: high-salt buffer, 0.5 M KCl, 10 mM Tris-HCl, pH 7.5, DTE as indicated, and 1 mM EDTA; low salt buffer, 0.1 M KCl, 10 mM Tris-HCl, pH 7.5, DTE as indicated, and 1 mM $MgCl_2$.

Skeletal muscle MLCK was prepared essentially as described by Crouch et al. (1981) with some modifications reducing the purification time. A batchwise adsorption to DEAE-cellulose and a stepwise desorption instead of the gradient desorption were employed. Dialysis whenever possible was substituted by gel filtration on Sephadex G-25 columns. The leading peak eluted from the hydroxyapatite column was pooled, $MgCl_2$ and $CaCl_2$ were added to 1 mM and 0.1 mM,

† From the Institut für Physiologische Chemie, Lehrstuhl I, Ruhr-Universität, 4630 Bochum 1, West Germany. *Received March 18, 1983.* Supported by the Deutsche Forschungsgemeinschaft He 594/13-2 and the Fonds der Chemie. A Model E analytical ultracentrifuge was provided by the Gesellschaft für Strahlen- and Umweltforschung mbH, München.

[1] Abbreviations: MLCK, myosin light chain kinase; CM, calmodulin; Ca^{2+}-CM, Ca^{2+}-saturated CM; LC2, light chain 2; MLCK·CM, 1:1 molar ratio complex of MLCK and Ca^{2+}-CM; FH_s, head fragment, spontaneously proteolytic; FH_t, head fragment, tryptic; FH_s·CM, 1:1 molar ratio complex of FH_s and Ca^{2+}-CM; FH_t·CM, 1:1 molar ratio complex of FH_t and Ca^{2+}-CM; FT, tail fragment; MRW, mean residue weight; EDTA, ethylenediaminetetraacetic acid; DTE, dithioerythritol; PMSF, phenylmethanesulfonyl fluoride; $NaDodSO_4$, sodium dodecyl sulfate; TPCK, tosyl-L-phenylalanine chloromethyl ketone; Cl_3CCOOH, trichloroacetic acid; GdmCl, guanidinium chloride; EGTA, ethylene glycol bis(β-aminoethyl ether)-*N*,*N*,*N*′,*N*′-tetraacetic acid.

0006-2960/83/0422-4316$01.50/0

respectively, and a second CM-Sepharose 4B chromatography (2.5 × 15 cm column, 40 mL/h) was performed in 40 mM triethanolamine hydrochloride, 100 mM NaCl, 0.5 mM DTE, 0.2 mM benzamidine, and 0.1 mM PMSF, pH 7.5 (buffer A), containing 0.1 mM $CaCl_2$ and 1 mM $MgCl_2$. MLCK was eluted by buffer A containing 0.5 mM EGTA instead of $CaCl_2$ and $MgCl_2$ and was stored at −20 °C after the addition of an equal volume of glycerol.

Fragments of MLCK Produced by an Endogenous Protease. MLCK eluted from the first CM-Sepharose 4B column of the routine preparation (ca. 30 mg) was equilibrated against 15 mM K_2HPO_4, 1 mM DTE, and 1 mM $CaCl_2$, pH 6.8, on a column of Sephadex G-25, incubated for 2 h at 30 °C, and then chromatographed on a hydroxyapatite column as usual except that 1 mM $CaCl_2$ was included in all buffers. The first eluting peak, after 1 mM $MgCl_2$ was added, was applied to a CM-Sepharose 4B column (see above). Approximately 50% of the applied material passed through. The bound material was desorbed by buffer A containing 0.5 mM EGTA. The unbound protein again was applied to a CM-Sepharose 4B column as above. The unbound fractions from this column were transferred into buffer A containing 0.5 mM EGTA by gel filtration. These unbound fractions (termed FT) and the combined fractions desorbed from the affinity columns by EGTA (termed FH_s) were stored at −20 °C after the addition of glycerol to 50%.

Tryptic Calmodulin Binding Fragment of MLCK. Six milligrams of purified MLCK was adsorbed onto CM-Sepharose 4B (1.6 × 10 cm) equilibrated with buffer A (without benzamidine) containing 1 mM $MgCl_2$ and 0.1 mM $CaCl_2$ at room temperature. After 30 min, 20 mL of trypsin (10 μg/mL, dissolved in the same buffer) was quickly pumped onto the column. After 15 min, the digestion was stopped by quickly pumping 20 mL of an ice-cold solution of soybean trypsin inhibitor (20 μg/mL in the same buffer) onto the column. After being further washed with 10 volumes of the above buffer at 4 °C, the material was eluted with buffer B containing 2 mM EGTA. The eluate was diluted 3-fold with H_2O and applied to a column of DEAE-Sephacel (1.6 × 5 cm), equilibrated against 40 mM triethanolamine hydrochloride, 0.2 mM benzamidine, 1 mM DTE, and 0.5 EGTA, pH 7.5. A linear gradient (100 mL) to 0.2 M NaCl was applied. Fractions (termed FH_t) containing only fragments of M_r ~36 000 judged by gel electrophoresis were pooled, concentrated on a second DEAE-Sephacel column by stepwise elution or on a small column of CM-Sepharose 4B (like above), and stored as described above.

Calmodulin was isolated from bovine brain according to Yazawa et al. (1980). A final fluphenazine–Sepharose 4B affinity chromatography was carried out as described by Charbonneau & Cormier (1979) instead of the gel filtration.

Phosphorylatable light chains (LC2) in the dephosphorylated form were isolated from myosin freshly purified from rabbit skeletal muscle according to Trayer & Perry (1966) and dephosphorylated according to Pemrick (1980). The light chains were further fractionated as described by Holt & Lowey (1975). Contaminating CM was removed by fluphenazine–Sepharose 4B affinity chromatography.

Fluphenazine–Sepharose 4B was prepared as described by Kakiuchi et al. (1981). Epoxy activation of Sepharose 4B was carried out as described by Sundberg & Porath (1974).

Calmodulin–Sepharose 4B (0.8–0.9 mg/g of gel) was prepared as described by Sharma et al. (1980). Coupling to divinyl sulfone activated Sepharose 4B was carried out at pH 9.5 in the presence of 50 μM $CaCl_2$.

Gel electrophoresis in the presence of $NaDodSO_4$ was carried out according to Weber & Osborn (1969) or Laemmli (1970).

For isoelectric focusing the method of O'Farrel (1975) was employed. *Protein* was determined by an automatized Lowry procedure (Lowry et al., 1951) with bovine serum albumin as the standard ($OD_{280,1\ mg/mL}$ = 0.660). CM determination was calibrated by a CM standard solution. Its concentration was established by an $OD_{276,1\ mg/mL}$ of 0.2 in the Ca^{2+}-free form and by amino acid analysis. MLCK determinations were calibrated via the OD given under Results.

MLCK activity assays were carried out at 30 °C in 40 mM Tris-HCl, pH 8.0, 8 mM $Mg(OAc)_2$, 100 μM $CaCl_2$, 1 mM DTE, 1 mM [γ-^{32}P]ATP (0.2 mCi/μmol), 1 μM CM, and 70 μM LC2 at appropriate dilutions of the enzyme (ca. 0.1 μg/mL). Aliquots were withdrawn repeatedly and analyzed for Cl_3CCOOH-precipitable radioactivity by the filter paper method of Corbin & Reimann (1975). For the steady-state kinetic analysis (K_m for CM, LC2, ATP; activation by Ca^{2+} and Mg^{2+}) the other components were held at standard conditions. Ca^{2+} was varied by employing 1 mM EGTA/Ca^{2+} buffers, and free Ca^{2+} was calculated as described by Kilimann & Heilmeyer (1982).

Amino Acid Analysis. Samples were either precipitated with 10% cold Cl_3CCOOH and washed with water or extensively dialyzed in EDTA-treated and boiled dialysis tubing against 0.1 M NH_4HCO_3 and lyophilized. Aliquots for spectra and protein determination were separated from the latter samples. To part of the samples were added thioglycolic acid and for quantitations norleucine as an internal standard prior to hydrolysis. Specified conditions are given in Table I. A Biotronik-6000 amino acid analyzer with one column system (0.6 × 25 cm, Durrum DC6 A resin) and lithium citrate buffers was employed.

Analytical ultracentrifugations were performed in a Beckman Model E equipped with electronic speed control, RTIC temperature control unit, and a photoelectric scanning system. Samples were freshly reduced by adding 2–5 mM DTE and equilibrated against the appropriate buffers by gel filtration on small columns of Sephadex G-25. Sedimentation velocity experiments were carried out at 60 000 rpm in double sector cells (12 mm) with quartz windows and Kel F centerpieces at 4.0 °C. Sedimentation equilibrium runs were carried out with column heights of ca. 3 mm at low (9000–12 000 rpm) and intermediate speed (15 000–22 000 rpm) and 4.0 °C in six channel cells (12 mm). Time to equilibrium was estimated as recommended by Teller (1973). Equilibrium scans were recorded at 280 nm in triplicate. Base-line scans were recorded after 5–6 h at 40 000 rpm and slowing down the speed to the original value without using the brake. Sedimentation coefficients were calculated from the inflection point positions r of the boundaries recorded in 16-min intervals by linear regression of log r vs. time. $s'_{20,w}$ values were calculated according to Svedberg & Pedersen (1940). Stokes' radii were calculated according to $R_{S,sed} = M(1 - \bar{v}_2\rho)/(6\pi\eta Ns)$ from M and the s value, with density ρ and viscosity η (in centipoise) of solvent,[2] and N as Avogadro's constant. Frictional ratios were obtained as $f/f_0 = R_{S,sed}/R_0$ with $R_0 = [3\bar{v}_2M/(4\pi N)]^{1/3}$.

Sedimentation equilibrium data, generally 30–35 c_r vs. r points with decreasing r spacing toward the bottom, obtained by point by point subtraction of the base-line values, were analyzed by two numerical techniques using a desk top computer (HP 85).[3] In the first treatment the c_r vs. r data were

[2] Index "1" for solvent (component 1) parameters omitted.

[3] Programs named SEDEQUI and SEPAM are available on request.

directly fitted by the function

$$c_r = \sum_{i=1}^{n} c_{im} \exp[\sigma_i(r^2 - r_m^2)/2]$$

with $\sigma_i = M_i(1 - \bar{v}_2\rho)\omega^2/(RT)$ as described by Haschemeyer & Bowers (1970). A simple peeling-off procedure [as described by Yphantis (1964)] was used to decide on n. This treatment yielded reliable values for the total meniscus concentration c_m and for σ_i of the smallest component present and a set of c_{im} and σ_i values for higher molecular weight components if present. In a second treatment, point average molecular weight moments were calculated from c_r vs. r data by using the c_m value from treatment I. The numerical techniques used were combinations of the methods described by Teller (1973) and Grant Kar & Aune (1974).

Densitometry of buffers and protein solution extensively dialyzed against the appropiate buffers was carried out at 4.0 ± 0.005 °C with a digital density meter of the mechanical oscillator type (chempro/PAAR DMA 60 + DMA 601) as described by Kratky et al. (1973). Instrument performance was checked with bovine serum albumin.

Analytical Gel Filtration. A column of Sephacryl S-300 (1.5 × 86 cm) equilibrated in high-salt buffer containing 0.5 mM DTE was performed at 4.0 ± 0.5 °C and 5 mL/h; 1-mL fractions were collected. Protein was monitored by UV absorbance, and the elution volume of MLCK was confirmed by activity measurement. Calibration was performed as described by Byers & Kay (1982). The Stokes radius $R_{S,gel}$ was estimated according to Siegel & Monty (1966).

Viscosity experiments were carried out with an Ubbelohde type microviscometer (130 mm capillary length, 1 mL outflow volume); temperature was maintained at 4.0 ± 0.001 °C. Repeated measurements were performed by means of a Viscotimer (Schott, FRG). Outflow times were between 148 and 160 s with a scatter of ±0.05 s. Protein solutions prepared like for the analytical ultracentrifugation experiments were clarified by centrifugation at 5000g and were successively diluted. Concentrations were measured for every dilution step. Data were treated by standard methods (Bradbury, 1970). A density correction for the protein was taken into account by adding 0.3 mL/g to uncorrected [η] values.

Far-UV CD spectra of protein solutions extensively dialyzed against the appropriate buffers were recorded at 20 °C by a Dichrograph Mark III (CNRS-Roussel Jouan/Jobin Yvon) by using quartz cells of 0.2–1-mm path length. The numerically smoothed and base-line corrected [θ] spectra were analyzed as described by Greenfield & Fasman (1969). A set of equations of the type $X_m = f_\alpha X_\alpha + f_\beta X_\beta + f_R X_R$ with X_α, X_β, and X_R as the [θ] values of corresponding reference spectra and X_m as the measured value was solved for the f values between 195 and 245 nm at 1-nm intervals by a least-squares technique. Reference spectra were the ones compiled by Yang et al. (1976). The condition $f_\alpha + f_\beta + f_R = 1$ always was included. A refinement of the fit concerning helix chain length dependence was performed as shall be described elsewhere.[4]

Results

Isolation of MLCK was optimized in a way that high purity was achieved within maximally 60 h, including the second CM-Sepharose 4B affinity chromatography. From 3 to 3.5 kg of muscle, 15–27 mg of >99% pure light chain kinase (see Figure 1) of a specific activity between 70 and 105 μmol·min^{-1}·mg^{-1} was obtained. The high specific activities are believed to be the result of an improvement and acceleration of the first enrichment steps and additionally of an optimized assay (see Materials and Methods). MLCK obtained after the hydroxyapatite chromatography slowly degraded proteolytically at 4 °C in the presence of Ca^{2+}. The second CM-Sepharose 4B chromatography led to an increase in the stability against proteolysis and removed degraded and inactive material still present. No degradation of the polypeptide chain was now observable upon storage for 2 weeks in the presence of 0.2 mM Ca^{2+} at 0 °C, and the activity decrease always was smaller than 50%. At −20 °C in 50% glycerol the enzyme was stable for at least 6 months.

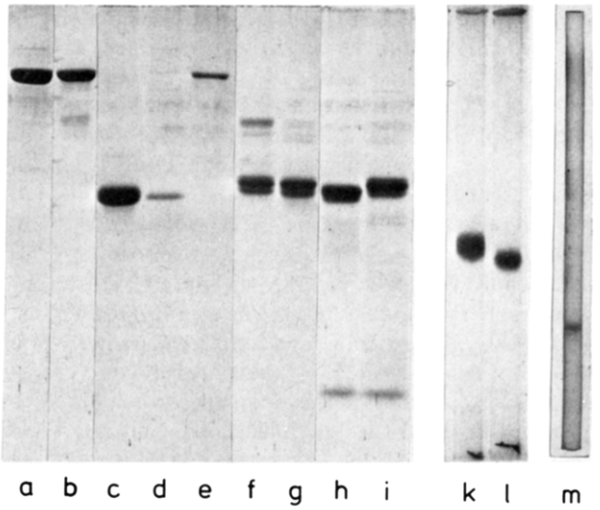

FIGURE 1: Characterization of MLCK, FH_s, FH_t, and FT by gel electrophoresis in the presence of $NaDodSO_4$ and isoelectric focusing of MLCK. In (a–i) samples were electrophoresed on 12.0% slab gels according to Laemmli (1970) and in (k) and (l) on 7.5% gels according to Weber & Osborn (1969). (a) MLCK (20 μg) freshly isolated; (b) MLCK (15 μg) after 1 week at 4 °C in the presence of 0.2 mM $CaCl_2$; (c) FH_s (20 μg); (d) FT (3 μg) showing a single band; (e) MLCK (4 μg) showing a single band; (f) FH_t (12 μg) as obtained before DEAE-Sephacel chromatography; (g) FH_t (15 μg) after DEAE-Sephacel chromatography; (h) FH_s·CM (20 μg) after 2 weeks at 0 °C in the presence of 0.2 mM $CaCl_2$; (i) FH_t·CM (20 μg) after storage like (h); (k) FH_s (10 μg); (l) FT (8 μg); (m) MLCK (10 μg) subjected to isoelectric focusing (pH decreasing from top to bottom).

The integrity and homogeneity of the MLCK were confirmed by (1) one band of M_r 84 000 ± 3000 on polyacrylamide gels in the presence of $NaDodSO_4$ (Figure 1), (2) one band upon isoelectric focusing, pI = 6 ± 0.5 (Figure 1), (3) homogeneous sedimentation profiles in the analytical ultracentrifuge at high and low ionic strength (see below), and (4) high specific activity with less than 1% of the maximal activity in the presence of 0.5 mM EGTA.

Kinetic analysis yielded K_m values for Mg·ATP of 330 μM, for LC2 of 18 μM, and for CM of 4.0 nM. Half-maximal Ca^{2+} activation in the presence of excess CM was observed at pCa 6.75 (Hill coefficient of 2.1). A single pH optimum at 8.0–8.5 and an optimal Mg^{2+} of 8 mM were found. All parameters were in good agreement with previously reported values (Pires & Perry, 1977; Blumenthal & Stull, 1980). The *UV spectrum* of MLCK showed a broad maximum at 276–278 nm, a shoulder at 290 nm typical for tryptophan, and some phenylalanine fine structure. The ratio OD_{280nm}/OD_{260nm} of 1.59 indicated the absence of more than traces of nucleotide material. An $OD_{278nm,1\ mg/mL}$ of 0.56 was determined based on amino acid analysis.

Proteolytic fragmentation of MLCK occurred spontaneously if the enzyme eluting from the first CM-Sepharose 4B column was incubated with millimolar $CaCl_2$. Two distinct fragments of M_r ~35 000 and 33 000 were obtained (Figure 1). From

[4] HP 85-program named CIDIC is available on request.

the succeeding hydroxyapatite column, the two fragments were eluted together like undegraded MLCK. A separation was possible as only the larger one (FH_s) bound to CM-Sepharose 4B. A second passage over CM-Sepharose 4B yielded an essentially pure M_r 33 000 fragment (FT). Both fragments were stable in the presence of 0.2 mM Ca^{2+} at 0 °C for 2 weeks.

A CM binding fragment was also produced by tryptic digestion of MLCK preadsorbed onto CM-Sepharose in order to protect the CM binding domain from proteolysis. At the trypsin concentration used, two types of fragments of M_r ~55 000 and 36 000 were produced which were still bound to the immobilized CM. Increasing the time of proteolysis led to a shift from M_r ~55 000 material to M_r 36 000. The tight binding of the fragments to the affinity matrix allowed an effective removal of protease and of nonbinding proteolytic fragments. The small amount of M_r ~55 000 fragments still present after digestion (Figure 1) could be separated from the smaller fragments by chromatography on DEAE-Sephacel. There was a broad peak of M_r 36 000 material which only in its ascending part contained the heavier fragments. From 6 mg of MLCK, 1.6 mg of >97% pure M_r 36 000 fragments (FH_t) was obtained, which were as stable as the fragments above.

Characterization of the Fragments Isolated. The CM binding fragments are termed FH (head fragment) with an index "s" for spontaneously proteolytic and "t" for tryptic. The non-CM binding fragment will be termed FT (tail fragment; for explanation see Discussion). Densitometry of gels performed according to Laemmli (1970) showed that FH_s consisted of two different polypeptides of M_r 34 500 and 35 500 present in a ratio of ca. 1:1. These two bands comprised >99% of the total protein, and no native MLCK was demonstrable. The specific activity of FH_s measured under standard conditions was ca. 12.6% of that of the MLCK from which it was isolated and 1.6% in the presence of 0.5 mM EGTA. A K_m value for LC2 of 17.5 μM was determined. The UV-absorbance spectrum of FH_s as compared with native MLCK was characterized by a significantly enhanced absorbance maximum at 276–277 nm ($OD_{277,1\ mg/mL}$ = 0.86) but a similar fine structure.

The FT fragment if subjected to electrophoresis according to Laemmli (1970) moved as one discrete band with a molecular weight very close to that of fragment FH_s. On gels according to Weber & Osborn (1969) a lower molecular weight of 33 500 was determined. The fragment was ca. 99% pure and showed no significant activity (maximally 0.2% of that of the native enzyme). The UV-absorbance spectrum showed a low-specific absorbance around 280 nm and indicated a very low amount of tryptophan.

The tryptic fragment FH_t (Figure 1) consisted of three polypeptides of M_r 37 000, 36 000, and 35 000 comprising ca. 10%, 60%, and 25% of the protein. The specific activity was 24.7% of that of MLCK as determined in the presence of Ca^{2+} and 0.2% in the presence of EGTA; the K_m value for LC2 was 17.8 μM. A reconstitution experiment was carried out by incubating equimolar amounts of FH_s and FT in the presence of excess LC2, CM, and Ca^{2+} 30 min prior to the start of the assay with ATP. The specific activity (based on FH concentration alone) increased in the presence of 100 μM Ca^{2+} and decreased in the presence of 0.5 mM EGTA. These changes were found to depend on the protein concentration: in the presence of Ca^{2+} the activity was 30.7% of the activity of MLCK at 0.26 μg/mL of total fragments and 56.3% at 2.6 μg/mL. In the presence of EGTA it decreased to 0.4% and 0.5%, respectively. Mixing of FH_t with FT at similar concentrations had no significant effect on the activities.

Table I: Amino Acid Composition of MLCK and the Fragments FH_s and FT[a]

	MLCK[b]	FH_s[c]	FT[c]	FH_s + FT[d]
Asx	79.8 ± 1.4	108.8 ± 2.5	65.9 ± 1.5	88.4
Thr	45.0 ± 1.4[e]	40.6 ± 0.7	38.2 ± 2.0	39.5
Ser	61.4 ± 1.4[e]	55.0 ± 1.6	64.2 ± 5.0	59.4
Glx	127.5 ± 1.8	104.8 ± 1.6	168.0 ± 1.9	134.8
Pro	83.9 ± 1.6	51.7 ± 2.8	106.9 ± 4.3	77.9
Gly	80.7 ± 1.8	54.5 ± 1.0	108.5 ± 1.4	80.2
Ala	97.4 ± 2.1	48.3 ± 2.6	113.9 ± 1.7	79.5
Val	50.5 ± 2.1[f]	55.0 ± 1.3	45.3 ± 1.0	50.4
Cys	16.5 ± 1.4[g]	ND	ND	
Met	15.6 ± 0.4[h]	31.2 ± 0.8[i]	9.3 ± 0.5[i]	20.8
Ile	38.2 ± 2.3[f]	43.8 ± 0.9	31.6 ± 0.6	38.0
Leu	71.2 ± 1.7	91.9 ± 1.8	65.8 ± 1.3	79.5
Tyr	11.5 ± 0.3[j]	17.7 ± 1.1[j]	10.0 ± 0.2[j]	14.0
Phe	31.9 ± 0.7	41.9 ± 1.3	29.3 ± 0.8	35.9
Lys	68.5 ± 1.2	67.1 ± 2.4	63.0 ± 2.0	65.2
His	15.4 ± 0.6	21.8 ± 0.4	13.5 ± 1.0	17.9
Arg	31.9 ± 0.4	39.7 ± 0.4	23.2 ± 0.4	31.9
Trp	7.2 ± 0.1[k]	9.7 ± 0.9[l]	2.1 ± 0.6[l]	6.1
NH_3	96.0 ± 5.7	ND	ND	
MRW	107	113	104	

[a] Values given are mol/10^5 g ± SEM. Samples were hydrolyzed in 6 N HCl at 110 °C. [b] Analysis done from two different preparations after 24, 48, and 72 h of hydrolysis in triplicate each. [c] Analysis done in duplicate after a 36-h hydrolysis. [d] Weight-average contents calculated by using the means of the molecular weights given in Table III. [e] Obtained by extrapolation to zero hydrolysis time. [f] Obtained from 72-h hydrolysis values. [g] Determined as cysteic acid after performic acid oxidation according to Hirs (1956). [h] Mean of the value obtained (as methionine sulfone) after performic acid oxidation and the one from thioglycolic acid containing samples. [i] Only from thioglycolic acid containing samples. [j] Mean of values from amino acid analysis and values determined spectrophotometrically according to Edelhoch (1967). [k] Mean of values determined spectrophotometrically and colorimetrically according to Messimo & Musarra (1972). [l] Determined only spectrophotometrically.

The amino acid composition of MLCK (Table I) was in close agreement with previously published data (Crouch et al., 1981), showing a typically high Pro content of ca. 9 mol %. A main difference is the lower Trp content which was determined spectrophotometrically and additionally by a colorimetric method. The amino acid analysis performed on the fragments FH_s and FT (Table I) showed a strikingly lower content of Asx and higher content of Glx in FT as compared with FH_s. The amounts of the small hydrophobic amino acids Pro, Gly, and Ala were twice as high in FT than in FH_s, the contents of all aromatic amino acids as well as of Met and Arg were drastically lower and those of the branched-chain amino acids Val, Ile, and Leu were slightly lower in FT as compared with FH_s.

Sedimentation Equilibrium Studies. All hydrodynamic experiments were carried out at 4.0 °C. For the native proteins partial specific volumes measured at this temperature (see below) were used for data treatment in order to avoid larger errors in the buoyancy terms.

Figure 2A shows a typical molecular weight distribution as a function of the local cell concentration for MLCK. Always some higher molecular weight material (M_r >250 000) was present but no material smaller than M_r 70 000. As indicated by the small increase in number- and weight-average molecular weights, the total cell concentration of material larger than M_r 70 000 was low. No change in the polypeptide homogeneity of the samples could be detected after the experiments by gel

Table II: Hydrodynamic Properties of MLCK, MLCK·CM, and CM [a]

	MLCK	MLCK·CM	CM	MLCK + CM
$\bar{v}_{2(4,l.s.)}$ (mL/g)	0.726 (0.004)	0.715 (0.005) 0.721[c]	0.706 (0.006)[b] 0.700 (0.004)[d]	0.720 (0.006) 0.722[e]
$\bar{v}_{2(20,l.s.)}$ (mL/g)	0.732[f]	0.721[f]		
$\bar{v}_{2(20,w)}$ (mL/g)	0.730[g]	0.726[g]	0.712[h] 0.707[i]	
M	70300 (1200)	87200 (1200)[j]	16720[k]	
$s_{20,w(l.s.)}$ (S)	3.03 (0.04)	3.63 (0.03)	1.74 (0.05)[l] 1.83 (0.05)[m]	3.02/1.77
$s_{20,w(h.s.)}$ (S)	3.13 (0.08)			
$[\eta]_{(l.s.)}$ (mL/g)	16.9 (0.4)	15.3 (0.5)	5.2 (0.4)[m]	14.0
$[\eta]_{(h.s.)}$ (mL/g)	16.4 (0.5)			
$R_{S,sed(l.s.)}$ (Å)	54.5 (1.3)	58.8 (1.5)	23.8 (1.0)[m]	
$R_{S,sed(h.s.)}$ (Å)	52.8 (1.9)			
$R_{S,gel(h.s.)}$ (Å)	51.6 (0.9)			
$f/f_{0(l.s.)}$	2.00	2.02	1.42[m]	
$f/f_{0(h.s.)}$	1.90			
$\beta \times 10^{-6}$	2.22 (0.08)	2.15 (0.07)	2.13 (0.14)[m]	
$\delta\beta^{n}$ (g/g)	2.4	3.8	1.04[m]	
$\delta_{calcd}{}^{o}$ (g/g)	0.42	0.43	0.46	
a/b $[\delta = \delta_{calcd}]^{p}$	12.0	11.6	4.4[m]	

[a] Conditions for values indexed (l.s.), low-salt (l.s.) buffer containing 0.5 mM DTE; conditions for values indexed (h.s.), high salt (h.s.) buffer containing 0.5 mM DTE. For MLCK·CM, 0.2 mM $CaCl_2$ was included in the low-salt buffer, and for MLCK + CM, 0.5 mM EGTA was included additionally. Stokes' radii R_S, frictional ratios f/f_0, and β were calculated directly from the values measured at 4 °C to avoid normalization errors. Values in parentheses are errors of the data (usually deduced from ±2 SE of measured data). [b] With 50 μM EGTA, no Ca^{2+}. [c] Calculated weight average, the value for Ca^{2+}-CM used. [d] With 0.2 mM $CaCl_2$. [e] Calculated weight average, the value for Ca^{2+}-free CM used. [f] Values obtained by the temperature correction $d\bar{v}_2/dT = 0.0004$ mL/(g·K) (Durchschlag & Jaenicke, 1982). [g] Calculated by amino acid composition. [h] Ca^{2+}- and Mg^{2+}-free CM, from Crouch & Klee (1980). [i] Ca^{2+}-CM, from Crouch & Klee (1980). [j] Obtained by adding molecular weight of Ca^{2+}-CM to the value measured for MLCK. [k] Calculated from the sequence. [l] With 0.5 mM EGTA. [m] With 0.2 mM $CaCl_2$. [n] Obtained via the β factor. [o] Calculated from the amino acid composition (see Discussion). [p] Mean of prolate axial ratios obtained from $[\eta]$ and $R_{S,sed}$ at the bracketed δ.

electrophoresis. Therefore, higher molecular weight material could only consist of N-mers of MLCK. To decide whether the N-mers are in reversible equilibrium with monomers of irreversibly aggregated or both, simultaneous runs at different loading concentrations were performed. The nonoverlap of corresponding molecular weight moment vs. concentration curves (Figure 2B) indicates the presence of material irreversibly polymerized. Gel filtration prior to the runs could reduce the percentage of higher molecular weight material but not completely abolish it. A local radius plot (Yphantis, 1964) in Figure 2C, done with the M_w and M_z data shown in Figure 2B, also shows no overlap of corresponding moments, which is a sufficient condition for some reversible polymerization. Direct curve fitting (treatment I; see Materials and Methods) of c vs. $r^2/2$ data from a total of 12 equilibrium runs at different speeds (see Materials and Methods) and loading concentrations between 0.1 and 0.9 mg/mL assuming a two-component mixture yielded a mean molecular weight of component 1 of 70 300.

A low-speed run (9000 rpm) with a 1:1 molar mixture of MLCK and Ca^{2+}-CM in low-salt buffer at a loading concentration of 0.45 mg/mL resulted in a minimum molecular weight of 84 400. This clearly showed that complex formation with calmodulin was almost complete even at the meniscus (concentration close to 0.2 mg/mL), and the stoichiometry was 1:1.

High-speed sedimentation equilibrium runs with fragments FH_s and FT in low-salt buffer gave molecular weights of 37 200 and 31 700, respectively. In both cases, some percents of higher molecular weight material were also present. The temperature-corrected $\bar{v}_2$ values calculated from amino acid composition (as given in Table III) were used.

Sedimentation Velocity and Viscosity Studies. Series of sedimentation velocity experiments with MLCK, CM, and MLCK-CM were performed at 4.0 °C between 0.2 and 1.5 mg/mL. The corresponding $s_{20,w}$ values obtained by extrapolation of the s' values normalized to water and 20 °C to zero concentration and the derived hydrodynamic data are given in Table II. In all cases only one symmetric boundary gen-

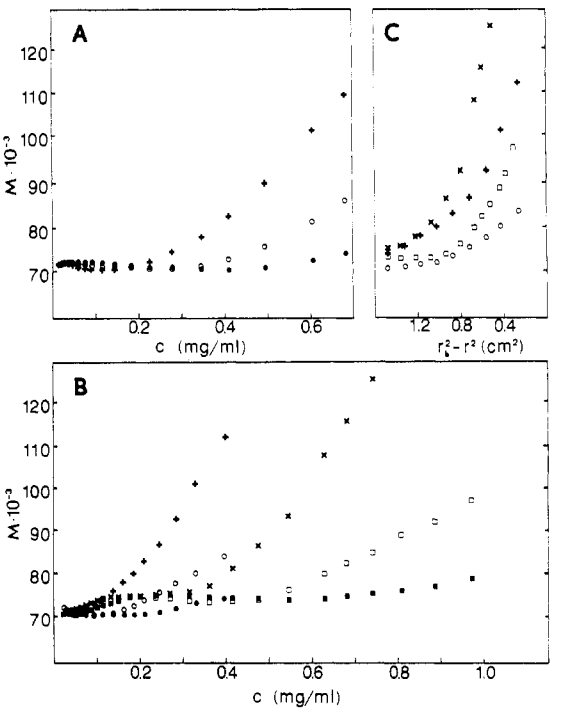

FIGURE 2: Sedimentation equilibrium analysis of MLCK. Plots of point average molecular weight moments M_n, M_w, and M_z vs. concentration in (A) and (B) and local radius plot in (C). Conditions: high-salt buffer and 0.2 mM DTE. (A) Loading concentration 0.1 mg/mL, 22 000 rpm; (●) M_n data; (○) M_w data; (+) M_z data. (B) 15 000 rpm; (●) M_n data; (○) M_w data; (+) M_z data at a loading concentration of 0.13 mg/mL; (■, □, ×) same moments at 0.34 mg/mL initial concentration. (C) M_w and M_z data from the experiments in (B) and same symbols.

Table III: Molecular Weights and Hydrodynamic Properties of the Proteolytic Fragments of MLCK and the Complexes with Ca^{2+}-CM[a]

	FH_t	FH_t·CM	FH_s	FH_s·CM	FT
M_r[b]	36500 ± 2000	53400[c]	35000 (2000)	53000[c]	33500 (2000)
M[d]			37200 (3000)		31700 (2700)
$\bar{v}_{2(20,w)}$[e] (mL/g)	0.735	0.726	0.735	0.726	0.726
$s_{20,w}$ (S)	3.08 (0.05)	3.56 (0.08)	3.11 (0.06)	3.73 (0.05)	1.81 (0.07)
$R_{S,sed}$	27.8	36.3	27.3	34.5	43.6
f/f_0[f]	1.27	1.46	1.25	1.40	2.07
δ_{max}[g] (g/g)	0.77	1.53	0.70	1.26	
δ_{calcd}[h] (g/g)	0.42	0.43	0.42	0.43	0.47
a/b [$\delta = \delta_{calcd}$][i]	2.7	5.0	2.5	4.2	14.3
a/b [$\delta = 0.8$][i]		3.4		2.7	11.3

[a] Conditions always were low-salt buffer containing 0.2 mM $CaCl_2$ and 0.5 mM DTE. For further explanations cf. Table II. [b] Determined by $NaDodSO_4$ gel electrophoresis according to Weber & Osborn (1969) (cf. Figure 1). [c] Obtained like for MLCK·CM (cf. Table II). [d] From two sedimentation equilibrium experiments in low-salt buffer plus 0.5 mM DTE at 22 000 rpm, and $\bar{v}_2$ temperature corrected as given under Table II. [e] Calculated from amino acid composition. [f] The mean of the differently obtained molecular weights was used for FH_s and FT. [g] Calculated assuming no asymmetry. [h] Calculated from amino acid composition. [i] Prolate axial ratios obtained from $R_{S,sed}$ at the bracketed δ.

erally representing more than 90% of the material loaded was observed. The remaining protein, obviously aggregated, sedimented faster, without forming a discrete boundary. A slightly negative slope of $s'_{20,w}$ vs. c plots in all three series (not shown) suggested that the analyzed boundary only represented nonaggregating protein.

MLCK alone showed a slightly higher $s_{20,w}$ value in high-salt buffer than in low-salt buffer. An unusually high Stokes radius of ca. 55 Å in low-salt buffer and a somewhat lower value in high-salt buffer indicating a slightly more compact structure under the latter conditions were found. To reinforce the high Stokes radius also reported by Crouch et al. (1981), analytical gel filtration was employed in addition. In high-salt buffer, a mean value out of four experiments differing by only 1.2 Å from the value deduced from sedimentation velocity was found. Adsorption prevented similar determinations at low-salt conditions. A significant increase in the sedimentation velocity was observed with MLCK·CM. A Stokes radius still higher than that of MLCK alone was calculated. Frictional ratios close to two were deduced for both MLCK and MLCK·CM from these sedimentation data. The hydrodynamic parameters of CM alone were in agreement with previously published data (Dedman et al., 1977; Crouch & Klee, 1980). Reversibility of MLCK·CM complex formation could be demonstrated by chelation of Ca^{2+} with 0.5 mM EGTA after a short prerun in the presence of Ca^{2+}. Components with $s_{20,w}$ values of ca. 1.8 and 3.0 (Table II) corresponding to CM and MLCK, respectively, reappeared.

Viscosity experiments with MLCK, MLCK·CM, and CM were performed at the same conditions and in the same concentration range as the sedimentation experiments. In this range, plots of the reduced viscosities η_{sp}/c vs. c were linear without concentration dependence (not shown); intrinsic viscosities are given in Table II. The most striking feature is the high intrinsic viscosity of ca. 17 mL/g for MLCK compared with values of 3–4 mL/g for normally hydrated globular proteins. Like in the sedimentation velocity a small difference between low-salt and high-salt buffers directed toward a more compact structure in high-salt buffer. For the 1:1 complex with Ca^{2+}-CM, an intrinsic viscosity lower by ca. 2 mL/g was observed. Addition of 0.5 mM EGTA to the complex instantaneously reduced the η_{sp}/c values by 1.3 mL/g. When the experiment was started with a 1:1 mixture in low-salt buffer in the presence of 50 μM EGTA and Ca^{2+} was added to 200 μM in excess, the reverse change was observed, suggesting a rapid reversible transition between dissociated and associated states. The intrinsic viscosity obtained for CM alone was 5.2 mL/g.

The proteolytic fragments and 1:1 molar mixtures of the head fragments with Ca^{2+}-CM were also subjected to sedimentation analysis at concentrations between 0.15 and 0.8 mg/mL. The corresponding $s_{20,w}$ values are given in Table III. Both CM-binding fragments, FH_t and FH_s, showed the same $s_{20,w}$ value; the fragment FT, however, although similar in molecular weight, sedimented drastically slower. As with the native enzyme, a low amount of faster sedimenting material was present. Equimolar amounts of Ca^{2+}-CM and FH_s or FH_t led to a significant increase of the $s_{20,w}$ values with still only one sedimentation boundary present. This suggests that both FH_s and FH_t, respectively, have formed a stable faster sedimenting complex with Ca^{2+}-CM in the concentration range examined. Under the same conditions equimolar amounts of FT and Ca^{2+}-CM sedimented independently from each other. The frictional ratios for the fragments FH were in the range found for globular proteins whereas FT had a frictional ratio still higher than that obtained for MLCK (cf. Table II).

Density measurements were performed on solutions of CM, MLCK, and a 1:1 mixture of MLCK and CM in the absence and presence of Ca^{2+}. The $\bar{v}_2$ values deduced and corresponding values calculated from amino acid composition are compiled in Table II for 4 and 20 °C. No variation of ϕ'_2 with protein concentration was found up to 3 mg/mL. For MLCK a close agreement of the observed $\bar{v}_2$ to the $\bar{v}_2$ calculated from amino acid composition (Cohn & Edsall, 1943) was found. Equimolar mixtures of MLCK and CM were measured in the presence of 50 μM EGTA and after the addition of saturating concentrations of $CaCl_2$. A buffer control was performed identically. Comparison of the measured $\bar{v}_2$ values with the weight-average $\bar{v}_2$ values calculated for molar 1:1 mixtures of MLCK and CM at 4 °C in the absence and presence of Ca^{2+}, respectively, shows a close agreement in the presence of EGTA but a value lower by 0.006 mL/g in the presence of Ca^{2+}. Complex formation therefore must have been accompanied by a positive density change of the solution.

Studies on Secondary Structures. Figures 3 and 4 show some of the CD spectra recorded in the far-UV region. $[\theta]$ values below are given in deg·cm²·dmol⁻¹. The CD spectrum of MLCK (Figure 3A) is characterized by a low overall ellipticity with a negative shoulder around 221 nm ($[\theta]_{221} = -4600$) and a minimum at 204 nm ($[\theta]_{204} = -7130$), suggesting a low amount of α helix and a large amount of "unordered" structure. Adding or chelating Ca^{2+} had no effect on the spectrum. The spectrum of FH_s indicates a larger amount of α helix and shows minima at 207 and 220 nm ($[\theta]_{202} = -3150$; $[\theta]_{220} = -6740$); in contrast the spectrum of FT does not suggest the presence of much α-helical structure. It is char-

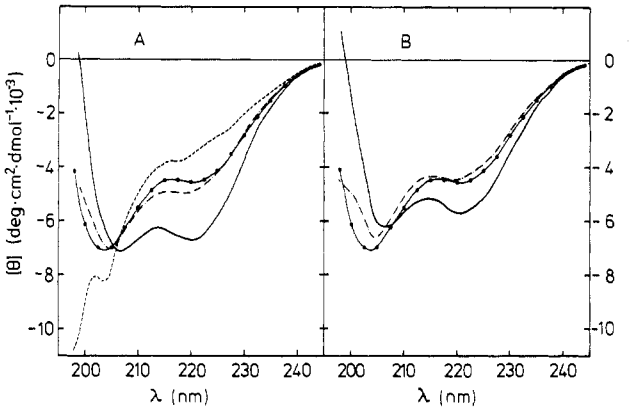

FIGURE 3: Far-UV CD spectra of native MLCK (●), FT [(---) in (A)], FH_s [(—) in (A)], and FH_t [(—) in (B)] recorded in low-salt buffer with 0.2 mM $CaCl_2$. (---) Residue number average spectrum calculated from the spectra of FH_s and FT in (A) and from FH_t and FT in (B).

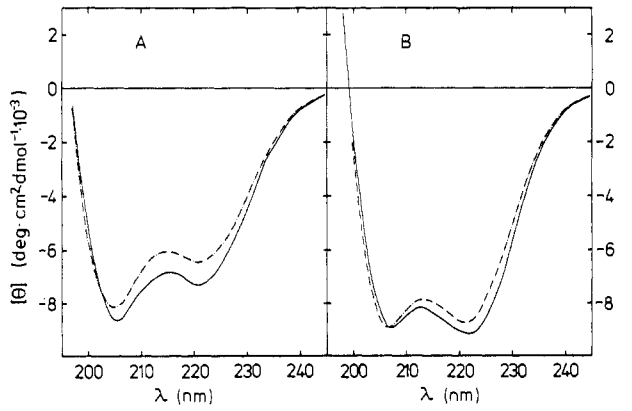

FIGURE 4: Far-UV CD spectra of approximate molar 1:1 mixtures of MLCK and CM (A) and FH and CM (B). For details see Table IV and Results. The continuous curves represent the spectra observed for the mixtures under associating conditions (i.e., the complexes) and the broken lines the spectra calculated for the mixtures by using the constituent spectra recorded under identical conditions.

acterized by a negative plateau around 217 nm, possibly suggesting β structure, a discrete minimum at 203 nm ($[\theta]_{203}$ = −8210), and a still more negative minimum below 198 nm. A residue number average spectrum calculated from the spectra of FH_s and FT is depicted in the same figure. Residue numbers per mole of protein were estimated by dividing the corresponding mean molecular weight by the MRW given in Table I. A close agreement with the spectrum of the native enzyme is obvious. FH_t shows a CD spectrum similar to that of FH_s (Figure 3B) but the minima, although at the same wavelengths, are smaller in absolute values ($[\theta]_{207}$ = −6300; $[\theta]_{230}$ = −5700). Again the calculated average spectrum with FT shows close resemblance to that of native MLCK. Figure 4 shows that Ca^{2+}-CM binding to MLCK or FH was accompanied by larger changes in secondary structure. In each experiment the concentrations of separate solutions of MLCK and CM were adjusted in Ca^{2+}-containing low-salt buffer at a molar ratio as finally desired for the mixture. Equal volumes of both solutions were mixed, EGTA was added to half of the constituent solutions and the mixture, and CD spectra of all six solutions were recorded. In the absence of conformational changes upon complex formation or the absence of interaction, the recorded spectrum of the mixture should be identical with the calculated composite spectrum. Calculation of the composite spectrum was carried out by using the residue number average (see above). Indeed, identical spectra were obtained

Table IV: α-Helix and β-Form Contents and Mean Chain Lengths of α Helices of MLCK, Its Fragments, and the Complexes with CM As Estimated from Far-UV CD Spectra[a]

polypeptide(s)	α helix ± SE (%)	β form ± SE (%)	$\bar{n}$ ± SE (residues)
MLCK	17 ± 1	3 ± 3	6.7 ± 0.4
Ca^{2+}-CM	59 ± 2	5 ± 2	8.4 ± 0.4
CM (Ca^{2+} free)	52 ± 2	10 ± 2	8.5 ± 0.5
MLCK·CM (measd)[b]	29 ± 2	9 ± 3	7.5 ± 0.8
MLCK·CM (calcd)[c]	24	3	7.4[d]
MLCK + CM (measd)[e]	24 ± 1	5 ± 2	7.3 ± 0.5
MLCK + CM (calcd)[f]	23	4	7.4[d]
FH_s	20 ± 1	7 ± 3	8.5 ± 0.4
FT	10 ± 2	6 ± 3	11.6 ± 1.2
FH_s·CM (measd)[g]	33 ± 1	10 ± 2	7.4 ± 0.3
FH_s·CM (calcd)[h]	30	6	8.4[d]

[a] All spectra were recorded in low-salt buffer, in the presence either of 0.2 mM $CaCl_2$ or of 0.2 mM $CaCl_2$ and 0.5 mM EGTA. The symbols for polypeptides and complexes are explained in the text and in Tables II and III. The values given are the means ± SE of two to four different spectra each. The standard error represents variation between the single spectra. Mean chain length $\bar{n}$ is used as by Chen et al. (1974). The values given for MLCK·CM and FH_s·CM do not exactly represent those of a 1:1 molar complex as a slight excess of MLCK and FH_s was present, respectively. [b] Weight ratio MLCK:CM of 0.22:1. [c] Calculated average for a mixture of Ca^{2+}-CM and MLCK at the same weight ratio. [d] Calculated as a weight average of α-helix fractions. [e] Same weight ratios as in footnote b, with uncomplexed mixture of MLCK and Ca^{2+}-free CM. [f] Calculated average for the same mixture. [g] Weight ratio CM:FH_s of 0.34:1. [h] Calculated average for the same mixture of Ca^{2+}-CM and FH_s.

in the presence of EGTA (not shown). In the presence of Ca^{2+}, however, the measured spectrum of MLCK·CM (Figure 4A) was significantly different from the calculated composite spectrum; the corresponding spectra of FH_s·CM also were different (Figure 4B), yet by a smaller degree. In both cases the minimum around 221 nm was more negative. With a mixture of FH_t and CM, we failed to demonstrate corresponding changes in ellipticity. The CD data of CM in the presence and absence of Ca^{2+} agreed with previously published data (Wolff et al., 1977; Richman & Klee, 1979).

In Table IV the α-helix and β-sheet contents and mean chain lengths estimated as given under Materials and Methods are compiled. An α-helix content of 17% and a low mean chain length were estimated for native MLCK. Fragment FH had a significantly higher α-helix content than FT. Weight-average α-helix and β-sheet contents for the mixtures of FH and FT close to the values of MLCK were calculated. The mean α-helix chain length calculated from these fragments was not consistent with the estimate for MLCK, but at low α-helix content this estimate is less reliable. Low β-sheet contents in all cases were estimated; however, uncertainty in these estimates generally is high. The analysis clearly showed ca. 5% increase in α-helix content upon complex formation between MLCK and Ca^{2+}-CM as well as ca. 6% increase in β-sheet content. For the complex between FH_s and Ca^{2+}-CM a smaller increase in α-helix and β-sheet content was found. In the absence of Ca^{2+}, the α-helix and β-sheet contents calculated for the mixture of MLCK and CM from the constituent contents agreed well with the values found for the real mixture, demonstrating the consistency of the CD spectrum analysis technique. By this technique, for the Ca^{2+}-free form of CM vs. the Ca^{2+}-saturated form a decrease in α-helix content by 7% and simultaneously an increasing β-sheet content were estimated.

Discussion

The molecular weight obtained from sedimentation equilibrium is lower than previously reported (Crouch et al., 1981), but a similar value of 73 000 can be calculated from the quantity $M(\partial\rho/\partial c_2)_\mu$ given by these authors and the buoyancy term from our own data after temperature and density correction. In contrast, we like others found a higher molecular weight value by gel electrophoresis (80 000 by Weber–Osborn gels and even 84 000 by Laemmli gels). As the hydrodynamic estimation is largely free from major errors provided the buoyancy term is measured, we have assumed the value of 70 300 to be close to the real molecular weight and have used it for all calculations.

Since the small amount of aggregated MLCK material always observed in sedimentation equilibrium experiments had molecular weights several times larger than that of the monomer, the monomer molecular weight could be reliably estimated. In sedimentation velocity runs the monomer sedimentation boundary was undisturbed by the faster sedimenting species. For the viscosity measurements a systematic error introduced by the polymerized material was unavoidable but should have been reduced by using high concentrations of DTE and examining the low protein concentration range.

It has been suggested that the complex of MLCK with Ca^{2+}-CM has a 1:1 stoichiometry (Crouch et al., 1981; Blumenthal & Stull, 1980; Adelstein & Klee, 1981). We can confirm this stoichiometry by the minimum molecular weight found at sedimentation equilibrium of a molar 1:1 mixture of Ca^{2+}-CM with MLCK, by the single homogeneous sedimentation boundary of this mixture, and by the Ca^{2+}-CM-activation curve measured at high MLCK concentrations (0.15 μM) which reached its plateau level at a 1:1 molar ratio.

The treatment of Scheraga & Mandelkern (1953), combining sedimentation and viscosity data in order to eliminate hydration, was employed to estimate the asymmetry of MLCK and its Ca^{2+}-CM complex. From the equation $\beta = (Ns[\eta]^{1/3}\eta \times 10^{-13})/[(1 - \bar{v}_2\rho)M^{2/3}]$ with $[\eta]$ in dL/g, β values of 2.22×10^{-6}, 2.15×10^{-6}, and 2.13×10^{-6} were obtained for MLCK, MLCK·CM, and CM, respectively, in low-salt buffer. When these β values are used, from the equation $[\eta] = \nu(\bar{v}_2 + \delta/\rho)$ an estimate of the hydration term is possible via the Shima factor ν, tabulated for the corresponding β values [e.g., in Yang (1961)]. Since the hydration terms obtained for prolate and oblate ellipsoid models (see δ_β in Table III) are unusually high, this way of estimating hydration and asymmetry seems to be invalid. As discussed by Kuntz & Kauzmann (1974), poor representation of the shape of the molecule by an ellipsoid model, differences in "effective hydration" between the two transport phenomena sedimentation and viscous flow, and a flexibility of the macromolecule can be the reasons.

Hydration therefore was calculated from amino acid composition according to Kuntz & Kauzmann (1974). The resulting values, δ_{calcd} in Table II, are close to the average hydration obtained for proteins by hydrodynamic techniques [0.53 ± 0.26 g/g (Squire & Himmel, 1979)]. When δ_{calcd} was used, axial ratios were determined either like above from $[\eta]$ or from f/f_0 via the Perrin shape factor F by using the equation $f/f_0 = F[1 + \delta/(\rho\bar{v}_2)]^{1/3}$. In all three cases (MLCK, MLCK·CM, and CM) the axial ratios obtained from f/f_0 are higher than those from $[\eta]$. This kind of data inconsistency in fact would be in accordance with the latter two reasons given above and was found by Kuntz & Kauzmann (1974) for most cases reexamined. The a/b values in Table II are the means of both estimates for a prolate ellipsoid, showing significant degrees of asymmetry for MLCK and MLCK·CM and a marked deviation from spherical shape also for CM.

Several criteria show that spontaneous proteolysis has led to two complementary fragments (FH_s and FT) still close to the native conformation and that cleavage must have occurred at a restricted region in the middle part of the polypeptide chain. (1) The amino acid contents of both fragments (Table I) add up closely to the contents calculated for MLCK. The small difference in the sum of molecular weights of the two fragments from that of the whole enzyme indicates that only 20 ± 5 residues of the native polypeptide are missing. A rather hydrophobic composition of Ala, Pro, Thr, Lys, Ser, and Gly (in decreasing frequency) can be estimated for these missing residues. (2) Only FH_s, the heavier one of these two fragments, expressed light chain kinase activity; its identical K_m value for LC2 with that of the holoenzyme indicates that cleavage did not affect the LC2-binding region. As the activity though to a smaller degree than that in the holoenzyme was Ca^{2+}-CM dependent and the fragment still bound to CM-Sepharose at concentrations below 1 μM, a major part of the Ca^{2+}-CM-binding and -sensitizing region must be located in this fragment and be relatively intact. The rise in specific activity found after reconstitution with the per se inactive fragment FT and the increase in the Ca^{2+}-CM activation strongly confirm complementarity of fragments and show that FT plays a role in the maintenance of activity and in Ca^{2+}-CM activation. (3) There is a close similarity of the residue number average CD spectrum calculated from the spectra of the fragments to the spectrum of the native enzyme. Similar evidence comes from the corresponding UV-absorbance spectra.

The tryptic fragment FH_t also showed all the above-mentioned properties. Attempts to increase the specific activity by reconstitution with fragment FT failed in this case. However, the Ca^{2+}-CM dependence of FH_t alone was already close to that of FH_s in the presence of FT. A polypeptide region located in FT close to the cleavage site and playing a role in Ca^{2+}-CM sensitization which is not cleaved off in the slightly larger fragment FH_t would account for this difference between FH_s and FH_t. The duplicate presence of this segment in FH_t and FT then could prevent reconstitution. The same would hold if such a peptide region were not directly involved in Ca^{2+}-CM binding but only in stabilizing a conformation of the active fragment essential for this property. For smooth muscle MLCK it was shown that both in the presence (Walsh et al., 1982a) and in the absence of CM (Walsh et al., 1980) the domain conferring Ca^{2+}-CM sensitivity can be split off, leading to a Ca^{2+}-CM-independent active fragment. In skeletal muscle MLCK both in the absence of CM (FH_s) and in the presence of immobilized CM (FH_t) under the conditions used, proteolytic cleavage between the catalytic domain and the Ca^{2+}-CM-binding region was somehow prohibited. In agreement with the findings in smooth muscle MLCK, however, calmodulin obviously had dictated a cleavage pattern different from that of the apoenzyme.

The terminology "head fragment" FH for the active Ca^{2+}-CM-binding fragments and "tail fragment" FT for the inactive fragment was introduced based on their hydrodynamic properties. FH_s and FH_t showed frictional ratios in the range characteristic for globular proteins (Table IV) (Squire & Himmel, 1979). Under the assumption of completely spherical particles, the maximum degrees of hydration (δ_{max} in Table IV) were calculated as ca. 0.75 g/g for the FH fragments and 1.25–1.53 for their complexes with Ca^{2+}-CM. The value of 0.75 g/g is in the normal range, but a doubling of this value upon Ca^{2+}-CM binding is unlikely, suggesting rather a change

in asymmetry. By use of the hydrations δ_{calcd} (Table III), which all were close to 0.4 g/g, prolate axial ratios of ca. 2.5 for the head fragments and ca. 4.5 for their complexes with Ca^{2+}-CM were obtained from f/f_0. The prolate model was virtually chosen. Axial ratios would remain constant if in fact Ca^{2+}-CM binding led to an increase in hydration to ca. 0.8 g/g.

For FT, a prolate axial ratio of 14.3 was obtained by using δ_{calcd} and of 11.3 by using 0.8 g/g for δ. A value for δ_{max} of 5.7 g/g, calculated for FT like above, would be only compatible with a completely unfolded polypeptide. It is concluded that FT in fact is highly asymmetric. For a hydration between 0.5 and 0.8 g/g, the long half-axis of FT can be calculated between 271 and 293 Å by using $a = R_h[(a/b)^2]^{1/3}$ with the hydrated radius as $R_h = R_0[1 + \delta/(\rho\bar{v}_2)]^{1/3}$. Whereas only a narrow range of error is left for hydration and asymmetry of FH, for FT an alternative confirmation of asymmetry is desirable. Therefore, electron microscopic experiments are in progress.

Further structural details can be deduced from the far-UV CD spectra, absorption spectra, and amino acid composition. The head fragments FH_s and FH_t have far-UV CD spectra resembling those of other intracellular enzymes with a relatively high α-helix content. Amino acid analysis and UV-absorbance spectrum indicates that FH_s contains most of the aromatic residues of the whole enzyme. The ca. 30% increase in tryptophan fluorescence observed by Johnson et al. (1981) upon interaction of MLCK with Ca^{2+}-CM thus means that a minimum of two of the four Trp found in the head fragment respond to Ca^{2+}-CM binding.

In CM alone, Ca^{2+} saturation leads to an increase in α-helical content to close to 60% (Table IV), a degree thought to be maximal from inspection of the primary structure. The further increase in α-helix and β-sheet content upon binding to MLCK, therefore, must be largely attributed to MLCK, there representing up to 50% of relative increase. The same holds for the increase in β-sheet content. As both α helix and β sheet represent highly condensed, hydrogen-bonded polypeptide structures, the ellipticity increase indicates a rise in packing density upon association. Our finding of a decrease in $\bar{v}_2$ at 4 °C upon Ca^{2+}-induced complex formation is compatible with an increase in packing density as well as with the burying of a larger hydrophobic surface area. The latter indeed may be important as the exposure of hydrophobic regions has been evidenced for Ca^{2+}-CM (LaPorte et al., 1980). Especially at low temperature, water forms highly ordered clathrate structures with lower packing density (close to that of ice) around hydrophobic structures, and the release of this structured water upon association indeed would lead to an apparent decrease of $\bar{v}_2$. Release of 4000 $Å^3$ of water from clathrate complexes of ρ 0.92 into bulk water with ρ 1.0 would comprise for ca. 50% of the observed change in $\bar{v}_2$. The corresponding buried surface area calculated assuming a water monolayer would be ca. 1400 $Å^2$, and this indeed is the range estimated for protein–protein interactions from crystal structures (Chothia & Janin, 1975).

For the tail fragment, from the presence of more than 11 mol % proline residues, obligate α-helix brakers [see Schulz & Schirmer (1979)], as well as from the CD spectrum, an α-helical backbone making up the above stated highly asymmetric structure can be excluded. The ca. 10% or 30 residues of α helix estimated could maximally span ca. 45 Å in length, as the rise per residue is 1.5 Å. Since no other sufficiently stable single-stranded structure is known, most of the length of ca. 280 Å must be spanned by the remaining ca. 280 non-α-helical residues by any other at least double-stranded

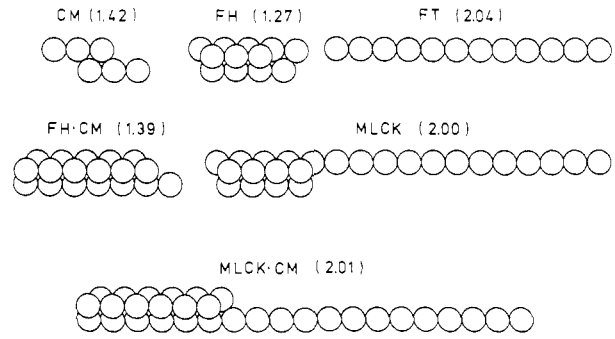

FIGURE 5: Bead models of MLCK, its proteolytic fragments FH_s and FT, and the complexes of FH_s and MLCK with CM constructed in a way to show closest agreement in calculated (values in parentheses) and experimentally established (cf. Tables III and IV) frictional ratios. For modeling all known hydrodynamic parameters were taken into account. Computer calculations were performed as described in the text. A (hydrated) unit sphere of 11.12-Å radius was chosen to account for (i) the previously estimated prolate shape of FT at 0.55 g/g hydration [a value virtually chosen, but close to δ_{calcd} (in Table IV)] and (ii) the volumes of the other species at hydrations close to 0.5 g/g (0.44–0.52 g/g). The hydrated volumes (in $Å^3$) thus used were 34 560, 144 000, 178 560, 69 120, 103 680, and 69 120 for CM, MLCK, MLCK·CM, FH_s, FH_s·CM, and FT, respectively. The single beads were arranged in hexagonal dense packing and rearranged by trial and error. Only the end to end arrangement of FH_s and FT resulted in frictional ratios as found for MLCK.

structure, with a consequent rise per residue of around 2 Å for a double-stranded and around 3 Å for a triple-stranded structure. Only two types of secondary structure account for this high rise per residue: the collagen-like and polyproline-like helical structures with 2.9-Å rise per residue and the β structure with 3.3 Å [see Schulz & Schirmer (1979)]. The high content of the amino acids Pro, Gly, and Ala known from sequence studies as major constituents of the collagen primary structure (Balian et al., 1972; Fietzek et al., 1973) indeed may suggest the presence of collagen-like segments. Because of their obligate requirement for Gly in every third position, a maximum collagenous chain length of ca. 300 Å may be estimated from the ca. 35 Gly present. Parallel alignment of three strands like in collagen is unlikely for a continuous polypeptide chain. Therefore antiparallel alignment of strands would have to be postulated, e.g., in a way found for synthetic poly(L-alanyl-L-prolylglycine) by Segal & Traub (1969). Additional stretches of a polyproline-like helix which has been evidenced as a parallel double helix in the IgG3 subclass (Marquart et al., 1980) may be assumed since Gly is not obligate in this structure. Finally a longer stretch of the fragment may be spanned by a β sheet built up from long antiparallel strands. The CD spectrum suggests a mixed structure perhaps containing all these elements. Such a structure might possess a significant amount of flexibility, thus providing the third explanation for the above discussed inconsistencies in hydrodynamic data, and might be suited for interactions with the elongated structures of myofilaments.

A refined model of the shape of MLCK, MLCK·CM, and the corresponding fragments was constructed by three-dimensional arrays of beads for which frictional ratios were calculated according to Bloomfield et al. (1967a,b) from $f_0 = 6\pi\eta R_0$ and $f = 6\pi\eta nr/(1 + (r/n)\sum_{i=1}^{n}\sum_{j=1}^{n} R_{ij}^{-1})$ $(i \neq j)$, with a number n of beads of a hydrated radius r and distance R_{ij} between beads i and j.

In Figure 5 one such model with good agreement in all frictional ratios is depicted, further confirming and illustrating the headed structure of MLCK. Lengths for MLCK of ca. 380 Å and for FT of ca. 270 Å and mean widths for FT of ca. 18 Å and for the head fragment of ca. 40 Å were deduced.

Ca^{2+}-CM binding leads to a length increase of the head part by ca. 40 Å.

Acknowledgments

We gratefully acknowledge the help and advice of Prof. Dr. Günther Snatzke in the CD measurements and thank Dr. Joseph H. Wissler for the use of the digital density meter. Our thanks are expressed to Friedhelm Vogel, Horst Korte, and Ulrich Wagner for expert technical assistance.

Registry No. MLCK, 51845-53-5.

References

Adelstein, R. S., & Klee, C. B. (1981) *J. Biol. Chem. 256*, 7501–7509.

Balian, G., Click, E. M., Hermodson, M. A., & Bornstein, P. (1972) *Biochemistry 11*, 3798–3806.

Bárány, K., Bárány, M., Gillis, J. M., Kushmerick, M. J. (1980) *Fed. Proc., Fed. Am. Soc. Exp. Biol. 39*, 1547–1551.

Bloomfield, V., Dalton, W. O., & Van Holde, K. E. (1967a) *Biopolymers 5*, 135–148.

Bloomfield, V., Van Holde, K. E., & Dalton, W. O. (1967b) *Biopolymers 5*, 149–159.

Blumenthal, D. K., & Stull, J. T. (1980) *Biochemistry 19*, 5608–5614.

Bradbury, J. H. (1970) in *Physical Principles and Techniques of Protein Chemistry* (Leach, S. L., Ed.) Part B, pp 99–145, Academic Press, New York.

Byers, D. M., & Kay, C. M. (1982) *Biochemistry 21*, 229–233.

Charbonneau, H., & Cormier, M. J. (1979) *Biochem. Biophys. Res. Commun. 90*, 1039–1047.

Chen, Y. H., Yang, J. T., & Chau, K. H. (1974) *Biochemistry 13*, 3350–3359.

Chothia, C., & Janin, J. (1975) *Nature (London) 256*, 705–708.

Cohn, E. J., & Edsall, J. T. (1943) *Proteins, Amino Acids and Peptides*, pp 370ff, Academic Press, New York.

Cooke, R., Franks, K., & Stull, J. T. (1982) *FEBS Lett. 144*, 33–37.

Corbin, J. D., & Reimann, E. M. (1975) *Methods Enzymol. 38C*, 287–290.

Crouch, T. H., & Klee, C. B. (1980) *Biochemistry 19*, 3692–3698.

Crouch, T. H., Holroyde, M. J., Collins, J. H., Solaro, R. J., & Potter, J. D. (1981) *Biochemistry 20*, 6318–6325.

Crow, M. T., & Kushmerick, M. J. (1982) *J. Biol. Chem. 257*, 2121–2124.

Dabrowska, R., Aromatorio, D., Sherry, J. M. F., & Hartshorne, D. J. (1977) *Biochem. Biophys. Res. Commun. 78*, 1263–1272.

Dabrowska, R., Sherry, J. M. F., Aromatorio, D. K., & Hartshorne, D. J. (1978) *Biochemistry 17*, 253–258.

Dedman, J. R., Potter, J. D., Jackson, R. L., Johnson, J. D., & Means, A. R. (1977) *J. Biol. Chem. 252*, 8415–8422.

Durchschlag, H., & Jaenicke, R. (1982) *Biochem. Biophys. Res. Commun. 108*, 1074–1079.

Edelhoch, H. (1967) *Biochemistry 6*, 1948–1954.

Edelman, A. M., & Krebs, E. G. (1982) *FEBS Lett. 138*, 293–298.

Fietzek, P. P., Rexrodt, F. W., Hopper, K. E., & Kühn, K. (1973) *Eur. J. Biochem. 38*, 396–400.

Glynn, I. M., & Chappel, J. B. (1964) *Biochem. J. 90*, 147–149.

Grant Kar, E., & Aune, K. C. (1974) *Anal. Biochem. 62*, 1–18.

Greenfield, N., & Fasman, G. D. (1969) *Biochemistry 8*, 4108–4116.

Haschemeyer, R. H., & Bowers, W. F. (1970) *Biochemistry 9*, 435–445.

Hirs, C. H. W. (1956) *J. Biol. Chem. 219*, 611–621.

Holt, J. C., & Lowey, S. (1975) *Biochemistry 14*, 4600–4609.

Johnson, J. D., Holroyde, M. J., Crouch, T. H., Solaro, R. J., & Potter, J. D. (1981) *J. Biol. Chem. 256*, 12194–12198.

Kakiuchi, S., Sobue, K., Yamazaki, R., Kambayashi, J., Sakon, M., & Kōsaki, G. (1981) *FEBS Lett. 126*, 203–207.

Kilimann, M. W., & Heilmeyer, L. M. G., Jr. (1982) *Biochemistry 21*, 1727–1734.

Kratky, O., Leopold, H., & Stabinger, H. (1973) *Methods Enzymol. 27*, 98–110.

Kuntz, I. D., Jr., & Kauzmann, W. (1974) *Adv. Protein Chem. 28*, 239–345.

Laemmli, U. K. (1970) *Nature (London) 227*, 680–685.

LaPorte, D. C., Wierman, B. M., & Storm, D. R. (1980) *Biochemistry 19*, 3814–3819.

Lowry, O. H., Rosebrough, N. J., Farr, A. L., & Randall, R. J. (1951) *J. Biol. Chem. 193*, 265–275.

Marquart, M., Deisenhofer, J., & Huber, R. (1980) *J. Mol. Biol. 141*, 369–391.

Messimo, L., & Musarra, E. (1972) *Int. J. Biochem. 3*, 700–704.

O'Farrel, P. H. (1975) *J. Biol. Chem. 250*, 4007–4021.

Pemrick, S. M. (1980) *J. Biol. Chem. 255*, 8836–8841.

Pires, E. M. V., & Perry, S. V. (1977) *Biochem. J.* 167, 137–146.

Richman, P. G., & Klee, C. B. (1979) *J. Biol. Chem. 254*, 5372–5376.

Scheraga, H. A., & Mandelkern, L. (1953) *J. Am. Chem. Soc. 75*, 179–184.

Schulz, G. E., & Schirmer, R. H. (1979) in *Principles of Protein Structure*, p 69, Springer-Verlag, New York.

Segal, D. M., & Traub, W. (1969) *J. Mol. Biol. 43*, 487–496.

Sharma, R. K., Wang, T. H., Wirch, E., & Wang, J. H. (1980) *J. Biol. Chem. 255*, 5916–5923.

Siegel, L. M., & Monty, K. J. (1966) *Biochim. Biophys. Acta 112*, 346–362.

Sobieszek, A., & Small, J. V. (1977) *J. Mol. Biol. 112*, 559–576.

Squire, P. G., & Himmel, M. E. (1979) *Arch. Biochem. Biophys. 196*, 165–177.

Sundberg, L., & Porath, J. (1974) *J. Chromatogr. 90*, 87–98.

Suzuki, H., Onishi, H., Takahashi, K., & Watanabe, S. (1978) *J. Biochem. (Tokyo) 84*, 1529–1542.

Svedberg, T., & Pedersen, K. O. (1940) *The Ultracentrifuge*, Oxford University Press, London.

Teller, D. C. (1973) *Methods Enzymol. 27*, 346–441.

Trayer, L. P., & Perry, S. V. (1976) *Biochem. Z. 345*, 87–100.

Walsh, M. P., Cavadore, J. C., Vallet, B., & Demaille, J. G. (1980) *Can. J. Biochem. 58*, 299–308.

Walsh, M. P., Dabrowska, R., Hinkins, S., & Hartshorne, D. J. (1982a) *Biochemistry 21*, 1919–1925.

Walsh, M. P., Hinkins, S., Flink, I. L., & Hartshorne, D. J. (1982b) *Biochemistry 21*, 6890–6896.

Walsh, M. P., Bridenbaugh, R., Hartshorne, D. J., & Kerrik, G. L. (1982c) *J. Biol. Chem. 257*, 5987–5990.

Weber, K., & Osborn, M. (1969) *J. Biol. Chem. 244*, 4406–4412.

Wolff, D. J., Poirier, P. G., Brostrom, C. O., & Brostrom, M. A. (1977) *J. Biol. Chem. 252*, 4108–4117.

Wolf, H., & Hofmann, F. (1980) *Proc. Natl. Acad. Sci. U.S.A. 77*, 5852–5855.

Yang, J. T. (1961) *Adv. Protein Chem. 16*, 323–400.

Yang, J. T., Chen, G. C., & Jirgensons, B. (1976) *Handbook of Biochemistry and Molecular Biology* (Fasman, G. D., Ed.) 3rd ed., Vol. III, pp 3-13, CRC Press, Cleveland, OH.
Yazawa, M., & Yagi, K. (1977) *J. Biochem. (Tokyo) 82*, 287-289.
Yazawa, M., Sakuma, M., & Yagi, K. (1980) *J. Biochem. (Tokyo) 87*, 1313-1320.
Yphantis, D. A. (1964) *Biochemistry 3*, 297-317.

Bovine Dentin Phosphophoryn: Composition and Molecular Weight†

W. G. Stetler-Stevenson and A. Veis*

ABSTRACT: The molecular weight of phosphophoryn, an acidic phosphoprotein unique to dentin matrix, has been difficult to determine because of a combination of neutral protease activities in this tissue and the intrinsic high charge density of the molecule. In this study, bovine dentin phosphophoryn (BDPP) was isolated by a procedure designed to prevent proteolysis. Bovine unerupted third molar powder was demineralized by ethylenediaminetetraacetic acid (EDTA). The EDTA-soluble phosphophoryn fraction was isolated and purified by sequential calcium chloride precipitation, gel filtration in sodium dodecyl sulfate ($NaDodSO_4$) containing buffer, anion-exchange chromatography, and finally gel filtration in 4 M guanidine hydrochloride (4 M Gdn·HCl) buffer. Sedimentation equilibrium, sedimentation velocity, and diffusion coefficient data, viscosity studies in a high ionic strength buffer, and $NaDodSO_4$ gradient gel electrophoresis data gave consistent results for the molecular weight of BDPP, all being in the range of 151 000–167 000. This range is much higher than any previously reported value. An anomalous behavior was observed in nongradient $NaDodSO_4$ gel electrophoresis. Dissociative analytical gel filtration chromatography in 4 M Gdn·HCl gave a molecular weight value of 100 000. This discrepancy was resolved by studying the viscosity of BDPP in 4 M Gdn·HCl which showed BDPP does not assume a true random-chain conformation in this solvent.

Phosphophoryns are major protein constituents of dentin extracellular matrix, accounting for as much as 50% of the noncollagenous proteins in some species. They are extremely rich in aspartyl, seryl, and phosphoseryl residues. Phosphophoryns bind calcium ions with high affinity (Lee et al., 1977; Zanetti et al., 1981) and can be preferentially precipitated by relatively high concentrations of calcium ion (Kuboki et al., 1979; Butler et al., 1981). They have been shown to markedly affect the in vitro crystallization of hydroxyapatite (Nawrot et al., 1976; DeSteno et al., 1975; Termine & Conn, 1976; Termine et al., 1980c). Autoradiographic (Weinstock & Leblond, 1973), biosynthetic (Dimuzio & Veis, 1978b; Maier et al., 1983), and analytical studies (Carmichael & Dodd, 1973) support the hypothesis that phosphophoryns are rapidly synthesized and secreted directly at the mineralization front. On the basis of these varied data, phosphophoryns have been postulated to play a number of important roles in normal dentinogenesis including nucleation and initial localization of calcium phosphate crystals within the hole regions of the collagen matrix (Butler, 1972; Veis, 1978; Dimuzio & Veis, 1978b; Glimcher, 1981; Veis et al., 1981).

However, discrepancies still exist in the literature concerning the molecular sizes and amino acid compositions of the phosphophoryns. Values for the molecular weight of bovine dentin phosphophoryn determined in earlier studies are on the order of 35 000–39 000 (Veis et al., 1972; Lee et al., 1977). Typically, these earlier studies failed to prevent proteolysis during demineralization and isolation procedures. Recent studies have shown that the strict prevention of proteolysis during isolation yields fetal bovine dentin phosphophoryn with a molecular weight on the order of 100 000 as determined by gel filtration in 4 M guanidine hydrochloride (Gdn·HCl) and sodium dodecyl sulfate ($NaDodSO_4$) gel electrophoresis (Termine et al., 1980b).

Recent studies of rat incisor dentin have shown that the rat incisor has at least two highly phosphorylated phosphoproteins (Dimuzio & Veis, 1978a,b; Linde et al., 1980; Butler et al., 1981). Different methods have given widely varying results for the molecular weights of these rat incisor phosphophoryns. For example, gel filtration chromatography in 3 M Gdn·HCl gave values of 65 000–71 000 for the molecular weights (Dimuzio & Veis, 1978a) whereas high-speed sedimentation equilibrium analysis performed in 0.1 M phosphate buffers containing 1 mM ethylenediaminetetraacetic acid (EDTA) at neutral pH showed no apparent concentration-dependent behavior and gave a molecular weight estimate of 30 000 (Jontell & Linde, 1977; Jontell et al., 1980). $NaDodSO_4$ gel electrophoresis has also been used to estimate the molecular weight of rat incisor phosphophoryns. When enzymatically dephosphorylated rat incisor phosphophoryns were run on $NaDodSO_4$ gel electrophoresis (7.5% acrylamide), a value of 72 000 was obtained for the molecular weight (Linde et al., 1980). When corrected for the addition of the phosphate, the estimate of the molecular weight became about 100 000. More recently, values of about 90 000 for the phosphorylated phosphophoryns have been obtained by using an acrylamide gradient $NaDodSO_4$ electrophoresis system (Butler et al., 1981). However, Jontell et al. (1982) have recently shown that rat incisor phosphophoryns behave anomalously in $NaDodSO_4$ gel electrophoresis systems as well as gel filtration chromatography in 6 M Gdn·HCl. Using sedimentation equilibrium analysis, these investigators also found nonideal behavior of the phosphophoryns from rat incisors in 1 M NaCl solutions. However, after dephosphorylation, these proteins showed ideal behavior in the analytical ultracentrifuge. The molecular weight of the dephosphorylated phosphophoryn was determined by this method to be 28 000. When corrected for

† From the Departments of Oral Biology and Molecular Biology (Biochemistry Program), Northwestern University Medical and Dental Schools, Chicago, Illinois 60611. *Received December 20, 1982.* This research has been supported by a grant from the National Institute for Dental Research (DE-01734).

* Address correspondence to this author at the Department of Oral Biology, Northwestern University Dental School.

0006-2960/83/0422-4326$01.50/0